Original Article

Association of increased epicardial adipose tissue derived from cardiac magnetic resonance imaging with myocardial fibrosis in Duchenne muscular dystrophy: a clinical prediction model development and validation study in 283 participants

Weifeng Yuan[1,2#^], Huayan Xu[1#], Li Yu[3], Lingyi Wen[1], Ke Xu[1], Linjun Xie[1], Rong Xu[1], Hang Fu[1], Bentian Liu[2], Ting Xu[1], Xiaoyue Zhou[4], Xiaoming Bi[5], Xiaotang Cai[6], Yingkun Guo[1^]

[1]Department of Radiology, Key Laboratory of Birth Defects and Related Diseases of Women and Children of Ministry of Education, West China Second University Hospital, Sichuan University, Chengdu, China; [2]Department of Medical Imaging, Clinical Medical College and The First Affiliated Hospital of Chengdu Medical College, Chengdu, China; [3]Department of Pediatric Cardiovascular Medicine, West China Second University Hospital, Sichuan University, Chengdu, China; [4]Siemens Healthineers Digital Technology (Shanghai) Co., Ltd., Shanghai, China; [5]Siemens Medical Solutions USA, Inc., Los Angeles, CA, USA; [6]Department of Rehabilitation, Key Laboratory of Birth Defects and Related Diseases of Women and Children of Ministry of Education, West China Second University Hospital, Sichuan University, Chengdu, China

Contributions: (I) Conception and design: Y Guo, W Yuan, H Xu; (II) Administrative support: Y Guo, H Xu, H Fu; (III) Provision of study materials or patients: T Xu, W Yuan, H Xu, K Xu; (IV) Collection and assembly of data: Y Guo, W Yuan, H Xu, L Yu, X Cai; (V) Data analysis and interpretation: W Yuan, H Xu, R Xu, H Fu, L Xie, L Wen, X Zhou, X Bi, B Liu; (VI) Manuscript writing: All authors; (VII) Final approval of manuscript: All authors.

[#]These authors contributed equally to this work.

Correspondence to: Yingkun Guo, MD, PhD. Department of Radiology, Key Laboratory of Birth Defects and Related Diseases of Women and Children of Ministry of Education, West China Second University Hospital, Sichuan University, No. 20, Section 3 South Renmin Road, Chengdu 610041, China. Email: gykpanda@163.com.

Background: Epicardial adipose tissue (EAT) contributes to inflammation and fibrosis of the neighboring myocardial tissue via paracrine signaling. In this retrospective study, we investigated the abnormal changes in the amount of EAT in male children with Duchenne muscular dystrophy (DMD) using cardiac magnetic resonance (CMR) imaging. Furthermore, we constructed and validated a nomogram including EAT-related CMR imaging parameter for predicting the occurrence of myocardial fibrosis in patients with DMD.

Methods: This study enrolled 283 patients with DMD and 57 healthy participants who underwent CMR acquisitions to measure the quantitative parameters of EAT, pericardial adipose tissue (PAT), paracardial adipose tissue, and subcutaneous adipose tissue. Late gadolinium enhancement (LGE) was performed to confirm myocardial fibrosis in patients with DMD. The DMD group consisted of 200 patients from institution 1 (the ratio of the training set and the internal validation set was 7:3) and 83 patients from four other institutions (the external validation set). Logistic and least absolute shrinkage and selection operator (LASSO) regression was used to select the optimal predictors and to develop and validate the nomogram model predicting LGE risk in the training set, internal validation set, and external validation set.

Results: Compared with those in healthy controls, some regional EAT thicknesses, areas, and global volumes were significantly higher in patients with DMD, and 41.7% of patients with DMD showed positive LGE. These LGE-positive patients with DMD showed significantly higher EAT volume (median 23.9 mL/m^3;

^ ORCID: Weifeng Yuan, 0000-0001-8336-6822; Yingkun Guo, 0000-0001-8437-9887.

P<0.001) and PAT volume (median 31.8 mL/m^3; P<0.001) compared with the LGE-negative patients with DMD. Age [odds ratio (OR) 2.0; P<0.001], body fat percentage (OR 1.3; P<0.001), and EAT volume (OR 1.4; P<0.001) were independently associated with positive LGE in the training set. The interactive dynamic nomogram showed superior prediction performance, with a high degree of the calibration, discrimination, and clinical net benefit in the training and validation of the DMD datasets. The area under the curve (AUC) values of the nomogram in the training set, internal validation set, and external validation set were 0.95 [95% confidence interval (CI): 0.91–0.98], 0.97 (95% CI: 0.92–0.99), and 0.95 (95% CI: 0.91–0.99), respectively.

Conclusions: The onset of LGE-based myocardial fibrosis was associated with EAT volume in patients with DMD. Additionally, the nomogram with EAT volumes showed superior performance in patients with DMD for predicting the occurrence of myocardial fibrosis.

Keywords: Duchenne muscular dystrophy (DMD); epicardial adipose tissue (EAT); cardiac magnetic resonance (CMR); myocardial fibrosis; prediction model

Submitted Jun 04, 2023. Accepted for publication Nov 10, 2023. Published online Jan 02, 2024.
doi: 10.21037/qims-23-790
View this article at: https://dx.doi.org/10.21037/qims-23-790

Introduction

Duchenne muscular dystrophy (DMD) is an X-linked recessive disease with an estimated worldwide incidence of about 1:3,500–6,300 live male births (1,2). Patients with DMD demonstrate a nonischemic pattern of myocardial fibrosis, which is associated with irreversible cardiac failure and mortality (3). Due to the fat replacement of muscle, limitations to progressive mobility, and side effects of glucocorticoid therapy, childhood obesity has gradually become one of the main complications of DMD (4). Moreover, the increased adiposity in the whole body has been shown to cause the onset of myocardial fibrosis in patients with DMD (5). Importantly, epicardial adipose tissue (EAT) is regarded as a key mediator of the deleterious effects of metabolic disorders on myocardial tissue and may contribute to the occurrence of myocardial fibrosis in obese patients (6,7). However, the levels of EAT and the association with myocardial fibrosis in patients with DMD have not yet been reported. Cardiac magnetic resonance (CMR) is a gold standard method for imaging adipose tissue, with excellent resolution in the soft tissues, and is the only imaging method for volumetric quantification of EAT that has been validated *in vitro* (8-11). In addition, late gadolinium enhancement (LGE) on CMR is the best noninvasive and nonionizing radiation-based imaging modality for detecting myocardial fibrosis in the early stages of cardiomyopathy in patients with DMD (12). However, gadolinium-based contrast agents (GBCAs) increase the risk of renal injury and deposition in the brain tissues in children due to their underdeveloped blood-brain barrier (13). Interestingly, the cine imaging in noncontrast CMR provides an alternate method for assessing myocardial fibrosis and reducing unnecessary gadolinium administration (14). Previous studies have indicated that LGE is correlated with a range of major adverse cardiovascular events such as death, heart failure, adverse left ventricular remodeling, and ventricular arrhythmia, and thus predicting LGE in the early stages of DMD is critical (3,15). Therefore, in this retrospective study, we hypothesized that the parameters of cine-based EAT are increased and that EAT can predict the occurrence of LGE-based myocardial fibrosis in children with DMD. The objectives of the study were to build and validate a novel prediction model. We present this article in accordance with the TRIPOD reporting checklist (available at https://qims.amegroups.com/article/view/10.21037/qims-23-790/rc).

Methods

Study enrollment

The study was conducted in accordance with the Declaration of Helsinki (as revised in 2013) and was approved by the China Ethics Committee of Registering Clinical Trials (ChiECRCT-20180107) and the Medical Ethics Committee of Sichuan University (No. K2019056) and registered in the Chinese Clinical Trial Registry (ChiCTR1800018340). Informed consent was obtained

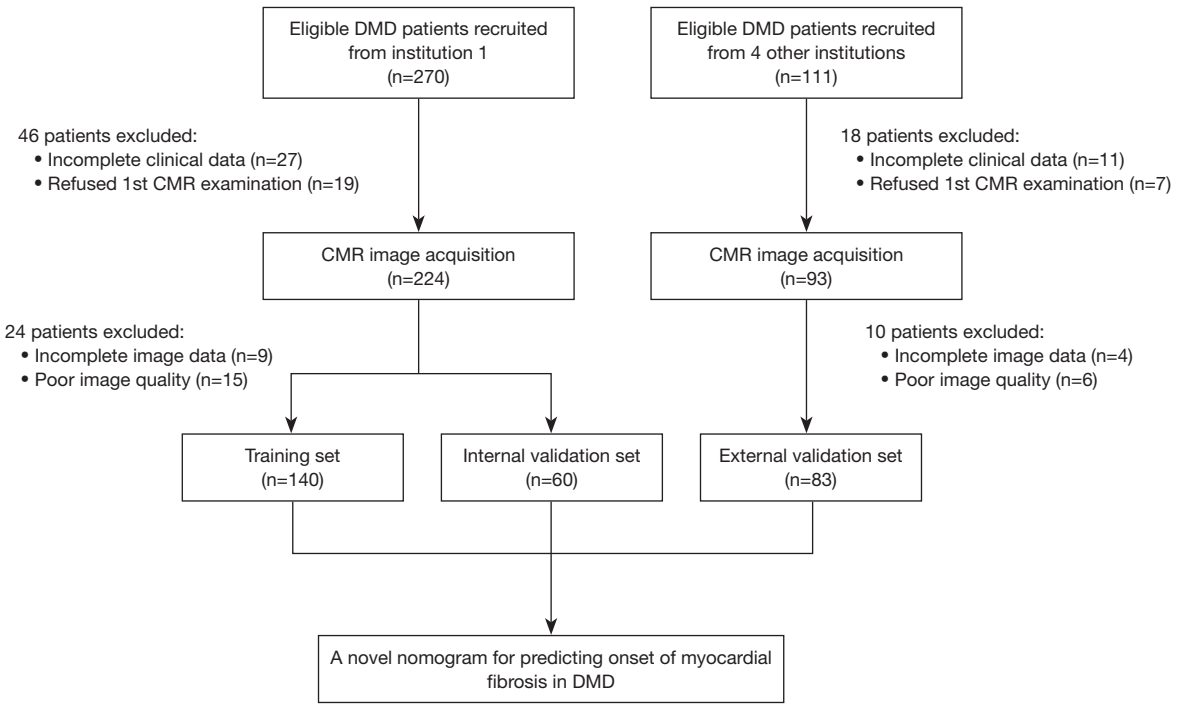

Figure 1 The flowchart of enrolled patients in the derivation and validation sets of the prediction model. DMD, Duchenne muscular dystrophy; CMR, cardiac magnetic resonance; LGE, late gadolinium enhancement.

from the patients' parents or their legal guardians. This multicenter study was conducted between September 2018 and September 2022 at the West China Second Hospital of Sichuan University and four other medical institutions, which were informed of and agreed with the study protocol (for details see the following: https://www.chictr.org.cn/showproj.html?proj=29770). The diagnosis of patients with DMD was strictly based on the guidelines for the diagnosis and management of DMD (16) and was confirmed by genetic testing that could identify the presence of deletions, duplications, or mutations in the dystrophin gene. Healthy participants without any history of cardiovascular disease or recent infection history were recruited as controls for this study. We measured the height, weight, heart rate, and blood pressure of healthy participants and conducted CMR imaging scans on them. After pre-experiment and sample size estimation (Appendix 1), 381 patients with DMD and 57 sex- and age-matched healthy participants were enrolled in this study. Due to refusal (written informed consent was not acquired from the enrolled participants before the CMR examination) or incomplete clinical data (missing rate was greater than 5%), 64 patients with DMD were excluded. After the first CMR acquisition, 34 patients with DMD were excluded due to incomplete image data (any one sequence or parameter was missing based on the procedure described in the CMR protocol section) or poor image quality (grade 1, according to the assessment method of the four-grade score for CMR image quality described in the MR image postprocessing and analysis section). Finally, 283 patients were enrolled as the DMD group, which consisted of 200 patients from the West China Second Hospital of Sichuan University (the ratio of the training set to the internal validation set was 7:3) and 83 patients from four other institutions (the external validation set) (*Figure 1*).

CMR protocol

All CMR imaging was performed on a 3T whole-body MR scanner (MAGNETOM Skyra, Siemens Healthineers, Erlangen, Germany) with an 18-channel body phased-array coil during repeated breath-holds. All the participants were examined in the supine position. After localization of the heart, cine images were acquired using the retrospectively electrocardiogram-gated, balanced steady-state free precession pulse sequences along the four-chamber long-axis slices and a stack of short-axis slices covering the whole

heart and the pericardial adipose tissue (PAT). All the short-axis cine images were obtained under the following parameters: field of view (FOV) =300×241 mm^2, repetition time =3.42 ms, echo time =1.48 ms, flip angle =34°, slice thickness =6 mm, acquisition matrix =126×224, and 25 frames per cardiac cycle. LGE images were acquired 5–10 min after intravenous injection at a dose of 0.1 mmol/kg gadolinium (Gadovist, Bayer Healthcare, Berlin, Germany). Instead of the standard segmented acquisition, a single-shot true fast imaging with steady-state free precession (trueFISP) acquisition with phase-sensitive inversion recovery (PSIR) reconstruction for a fast overview and a prototype single-shot PSIR with motion correction (MOCO PSIR) sequences (17) (work-in-progress, WIP #1325; Siemens Healthineers) for the high-resolution LGE imaging were used to reduce the influence of the motion. Corresponding parameters for the fast overview single-shot trueFISP and high-resolution MOCO PSIR were as follows: FOV =340×340/340×340 mm^2, repetition time =2.55/2.73 ms, echo time =1.09/1.15 ms, flip angle =55°/40°, slice thickness =8/8 mm, and acquisition matrix =116×192/136×240.

MR image postprocessing and analysis

MR image analysis was carried out using the commercially available CVI[42] software (Circle Cardiovascular Imaging Inc., Calgary, AB, Canada). The maximum transverse diameters and contours of the adipose tissue were manually drawn at the end-diastolic phase in the short-axis and long-axis four-chamber images. The thickness and area of each region covering the whole heart and the PAT were automatically calculated with the software (9,18). The border between EAT and PAT was visually delineated in all the slices (19). Total PAT and EAT volumes were obtained by summing the areas traced from all the short-axis slices and multiplying the slice thickness, as previously described (19,20). EAT consisted of adipose tissue in the left atrioventricular groove (AVG), right AVG, anterior interventricular groove (IVG), superior IVG, inferior IVG, and the right ventricular free wall (RVFW) as shown in the representative CMR images of the patients with DMD with increased EAT volume and the onset of LGE-based myocardial fibrosis (*Figure 2*). The measurements were performed in the end-diastolic phase on the basal short-axis plane at the end level of the papillary muscles and on the horizontal long-axis plane. EAT areas and thicknesses in the anterior IVG, left AVG, and right AVG were measured on the horizontal long-axis plane; meanwhile, EAT areas and thicknesses in the superior IVG, inferior IVG, and RVFW were measured on the basal short-axis plane (21). In the evaluation of LGE, positive LGE was considered to be presence of subepicardial or midmyocardial hyperenhancement according to visual inspection. The DMD group was divided into the LGE-negative and LGE-positive groups based on the absence and presence of abnormal delayed enhancement, respectively. The LGE and adipose tissue parameters were assessed by two experienced radiologists with more than 3 years of experience in CMR diagnosis. Intraobserver reliability was measured by comparing the measurements of a single radiologist for 30 randomly selected cases at two different time points within an interval of 2 weeks. The interobserver reliability was estimated by comparing the measurements of the two radiologists that were calculated in a blinded manner. An assessment method of the four-grade score was carried out for CMR image quality as follows: extensive artifacts with poor image quality, grade 1; moderate artifacts not disturbing image analysis, grade 2; mild artifacts with good image quality, grade 3; and absence of artifacts with excellent image quality, grade 4. Only images assessed as grade ≥2 were then included.

Statistical analysis

The normality and variance homogeneity of the measurement data were analyzed using the Kolmogorov-Smirnov test and Levene test, respectively. Data with a normal distribution and homogeneity of variance were compared using one-way analysis of variance (ANOVA), paired-samples *t* test, and least significant difference (LSD) *t*-test. The nonnormally distributed data were compared using the Mann-Whitney test and the Kruskal-Wallis test. The statistical significance of the differences between groups was assessed using the chi-squared test or Fisher exact probability method. Intraobserver and interobserver reliabilities were evaluated using intraclass correlation coefficients. Binary logistic regression analysis was performed to establish a prediction model based on the Akaike information criterion. Least absolute shrinkage and selection operator (LASSO) regression was used to screen variables included in the prediction model to reduce possible collinearity. The calibration plots and Brier scores were used to evaluate the calibration of the nomogram. Harrell C-statistic was used to evaluate the discrimination of the nomogram and calculate the area under the curve

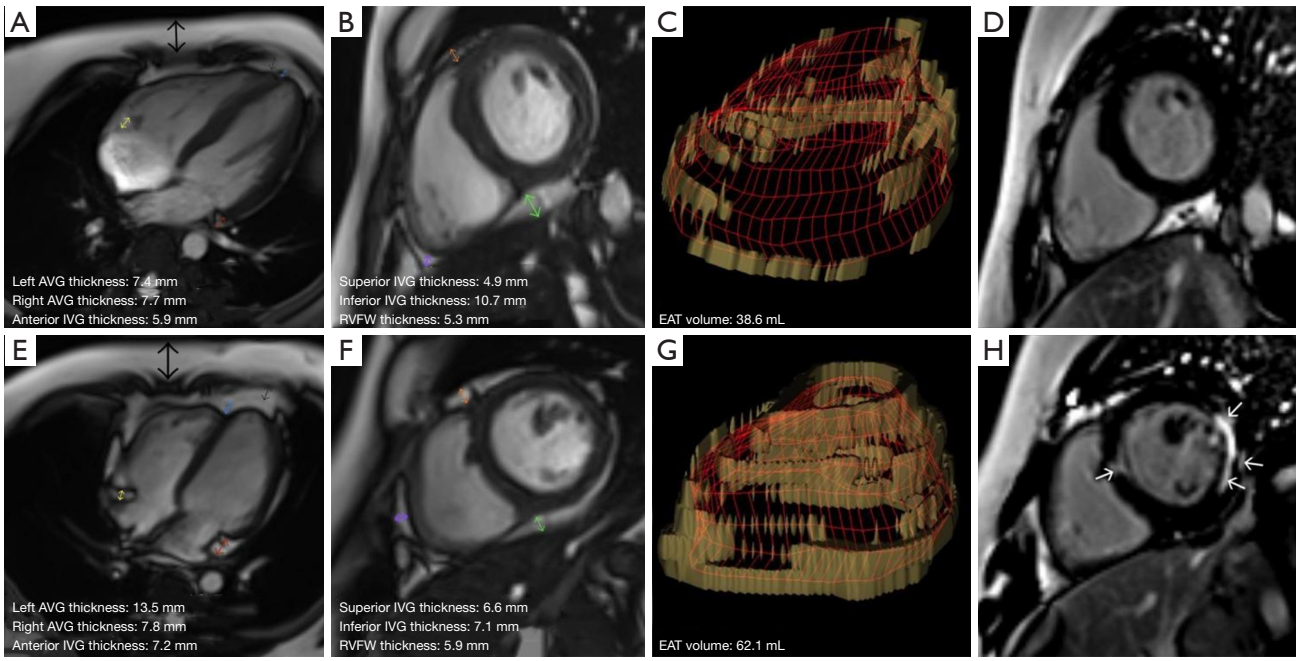

Figure 2 The CMR images in two 13-year-old boys with DMD. (A-D) An LGE-negative patient and (E-H) an LGE-positive patient. (A,E) Images from the four-chamber long-axis view in end diastole showing the EAT in the left AVG (red arrows), right AVG (yellow arrows), anterior IVG (blue arrows), paracardial adipose tissue (gray arrows), and subcutaneous adipose tissue (black arrows). (B,F) The images of the short-axis view in end diastole showing EAT in the superior IVG (orange arrows), inferior IVG (green arrows), and RVFW (purple arrows). (C,G) Reconstructions of the EAT volumes (brown areas). The red reticulate sections represent the epicardium. (D) An LGE image suggesting no myocardial fibrosis in the left ventricular wall. (H) An LGE image suggesting myocardial fibrosis in the left ventricular free wall (white arrows). EAT, epicardial adipose tissue; LGE, late gadolinium enhancement; DMD, Duchenne muscular dystrophy; AVG, atrioventricular groove; IVG, interventricular groove; RVFW, right ventricular free wall; MR, cardiac magnetic resonance.

(AUC) values for the training set, internal validation set, and external validation set. Decision curve analysis (DCA) was performed to evaluate the clinical applicability of the nomogram and display the clinical net benefit at different risk threshold probabilities. A P value <0.05 was considered statistically significant. SPSS 26.0 (IBM Corp., Armonk, NY, USA), PASS version 11.0 (NCSS, Kaysville, UT, USA), and R package version 3.5 (The R Foundation for Statistical Computing, Vienna, Austria) were used to complete statistical analyses.

Results

Baseline characteristics of the study participants

The clinical data of the patients in the DMD group (N=283) and the healthy participants in the control group (N=57) are shown in *Table 1*. There were no significant differences in age, sex, heart rate, systolic blood pressure, diastolic blood pressure, or left ventricular myocardial mass indexed to body surface area between the two groups (P>0.05). Compared with the control group, the DMD group showed statistically higher values in body mass index (median 18.1 kg/m^2; P<0.001) and body fat percent (BFP; median 19.0%; P<0.001) and statistically lower values in left ventricular ejection fraction (mean 60.8%; P<0.05), left ventricular end-systolic volume indexed to body surface area (median 22.0 mL/m^2; P<0.05), and left ventricular end-diastolic volume indexed to body surface area (median 57.5 mL/m^2; P<0.001). Additionally, 41.7% of patients with DMD showed abnormal delayed enhancement, and all of these patients (the same 41.7%) showed positive LGE in the free wall segments, while 6.7% of patients additionally showed positive LGE in the septal segments.

Quantitative parameters of EAT

The quantitative parameters (indexed to height^3) of the

Table 1 Baseline characteristics of the study participants

Parameter	Healthy controls (n=57)	DMD (n=283)	P value	DMD (n=283)		
				LGE (–) (n=165)	LGE (+) (n=118)	P value
Age, years	9.0 (7.0–10.5)	8.0 (7.0–10.0)	0.081	7.0 (7.0–8.0)	10.0 (8.0–13.0)	<0.001
Males, %	100.0	100.0	–	100.0	100.0	–
BMI, kg/m^2	16.7 (15.1–18.0)	18.1 (16.2–22.5)	<0.001	17.7 (16.1–20.8)	19.3 (16.4–24.3)	0.014
BFP, %	16.3 (14.0–19.4)	19.0 (15.5–24.7)	<0.001	17.2 (14.7–19.5)	25.4 (19.9–28.4)	<0.001
Heart rate, bpm	92.0 (78.0–98.5)	92.0 (85.0–102.0)	0.092	92.0 (84.5–103.5)	92.5 (85.8–100.3)	0.890
LVEF, %	62.6±3.8	60.8±4.2	0.005	61.3±4.6	60.2±3.7	0.044
LVESVI, mL/m^2	24.5 (21.8–26.9)	22.0 (18.9–25.5)	0.003	21.9 (19.2–25.3)	22.4 (18.7–25.9)	0.954
LVEDVI, mL/m^2	63.7 (58.3–70.1)	57.5 (51.3–63.7)	<0.001	57.8 (52.4–63.7)	56.1 (49.3–63.9)	0.172
LVMI, g/m^2	32.0 (27.6–37.0)	30.7 (28.1–34.4)	0.281	30.4 (28.1–34.3)	31.7 (28.2–34.6)	0.166
SBP, mmHg	104.0 (94.0–110.5)	103.0 (99.0–108.0)	0.496	104.0 (99.0–107.0)	103.0 (99.0–109.0)	0.631
DBP, mmHg	65.0 (52.5–73.5)	65.0 (60.0–73.0)	0.235	64.0 (58.0–72.5)	65.0 (61.0–73.0)	0.216
Creatine kinase, U/mL	–	12.7 (10.4–15.6)	–	13.1 (12.0–16.7)	10.9 (9.5–15.0)	<0.001
Glucocorticoid duration, years	–	2.7 (1.5–3.6)	–	2.5 (1.5–3.2)	3.0 (1.5–4.3)	0.007

Continuous variables are expressed as the mean ± standard deviation for parametric variables or as the median with interquartile range for nonparametric variables. DMD, Duchenne muscular dystrophy; LGE, late gadolinium enhancement; BMI, body mass index; BFP, body fat percentage; LVEF, left ventricular ejection fraction; LVESVI, left ventricular end-systolic volume indexed to body surface area; LVEDVI, left ventricular end-diastolic volume indexed to body surface area; LVMI, left ventricular myocardial mass indexed to body surface area; SBP, systolic blood pressure; DBP, diastolic blood pressure.

EAT, PAT, and subcutaneous adipose tissues in the healthy controls, the LGE-negative group, and the LGE-positive group are shown in *Table 2*. The patients in the DMD group showed increased left AVG thickness, left AVG area, inferior IVG area, PAT volume, and EAT volume compared with the control group (P<0.05). Furthermore, the LGE-positive group showed a significantly higher PAT volume (median 31.8 mL/m^3; P<0.001) and EAT volume (median 23.9 mL/m^3; P<0.001) compared with the LGE-negative group. The intraclass correlation coefficients of the adipose tissue quantitative parameters for the intraobserver and interobserver reliability are shown in Table S1. The thickness and area of EAT and paracardial adipose tissue, the volume of EAT and PAT, and the thickness of subcutaneous adipose tissue showed good reliability.

Nomogram model for predicting LGE in DMD

The optimal predictors of LGE-based myocardial fibrosis in DMD were selected based on the best lambda range after cross-validation in LASSO regression (*Figure 3A,3B*). The parameters including age (OR 2.0; P<0.001), BFP (OR 1.3; P<0.001), and EAT volume indexed (EATVI; OR 1.4; P<0.001) were independently associated with positive LGE in the training set and a novel interactive dynamic nomogram was established (*Figure 3C*). The regression equation was as follows: Logit(P) = –18.563 + 0.679 × Age + 0.244 × BFP + 0.352 × EATVI. The predictors and LGE occurrence have been compared among all the sets in *Table 3*. The Brier scores of the prediction model were in in the training set, internal validation set, and external validation set were 0.09, 0.06, and 0.09, respectively, which was consistent with the indication of superior goodness of fit and relatively small error in the calibration plots (*Figure 4A*). The AUC values of the nomogram in the training set, internal validation set, and external validation set were 0.95 (95% CI: 0.91–0.98), 0.97 (95% CI: 0.92–0.99), and 0.95 (95% CI: 0.91–0.99), respectively (*Figure 4B*), and higher than those of the single variable in the DeLong test, showing good discrimination of the model in all sets. DCA results showed superior clinical applicability of the nomogram because the net benefit remained positive value even if the risk threshold probability reached a maximum value (*Figure 4C*).

Table 2 Comparison of the quantitative parameters of adipose tissue

Parameter	Healthy controls (n=57)	DMD (n=283)	P value	DMD (n=283)		
				LGE (–) (n=165)	LGE (+) (n=118)	P value
PAAT thickness indexed, mm/m^3	3.5 (2.7–4.5)	3.6 (2.8–4.6)	0.602	3.6 (2.8–4.6)	3.6 (2.8–4.9)	0.835
EAT thickness indexed, mm/m^3						
Left AVG	1.9 (1.4–2.9)	2.4 (1.7–3.6)	0.003	2.3 (1.7–3.5)	2.5 (1.7–3.6)	0.668
Right AVG	3.5 (2.8–4.9)	3.7 (2.9–4.9)	0.722	3.6 (2.8–4.6)	3.9 (2.9–5.1)	0.234
Anterior IVG	1.7 (1.3–2.2)	1.8 (1.4–2.2)	0.609	1.7 (1.4–2.2)	1.8 (1.4–2.3)	0.391
Superior IVG	2.7 (2.0–3.4)	2.8 (2.1–3.7)	0.701	2.7 (2.1–3.6)	2.8 (2.2–3.7)	0.488
Inferior IVG	1.5 (1.2–2.2)	1.5 (1.2–2.2)	0.864	1.5 (1.2–2.2)	1.6 (1.2–2.3)	0.659
Right ventricular free wall	2.4 (2.0–3.3)	2.4 (1.9–3.2)	0.729	2.4 (1.9–3.2)	2.5 (1.9–3.3)	0.534
SAT thickness indexed, mm/m^3	3.8 (2.6–4.7)	3.8 (2.7–4.8)	0.761	3.7 (2.7–4.7)	4.0 (2.8–4.9)	0.427
PAAT area indexed, mm^2/m^3	447.8 (370.3–637.4)	467.4 (377.6–644.6)	0.675	466.0 (372.6–644.1)	480.8 (392.1–650.6)	0.404
EAT area indexed, mm^2/m^3						
Left AVG	48.7 (39.3–65.0)	58.6 (46.9–75.9)	<0.001	55.8 (46.2–74.3)	60.7 (48.1–77.1)	0.235
Right AVG	67.5 (54.6–81.5)	68.6 (54.3–85.8)	0.819	67.9 (54.0–84.7)	69.3 (54.3–86.8)	0.486
Anterior IVG	71.9 (53.0–93.9)	73.9 (54.3–94.0)	0.833	72.8 (53.6–91.6)	75.9 (55.9–96.1)	0.463
Superior IVG	46.7 (36.4–69.7)	48.3 (36.3–68.5)	0.822	48.3 (35.1–66.7)	48.5 (36.7–73.3)	0.485
Inferior IVG	30.4 (21.8–45.1)	37.9 (26.7–51.3)	0.007	36.4 (26.2–47.6)	39.2 (28.2–55.1)	0.226
Right ventricular free wall	97.9 (73.3–122.6)	98.8 (76.4–126.0)	0.878	98.8 (76.2–123.3)	98.4 (79.7–138.4)	0.642
PAT volume indexed, mL/m^3	23.1 (16.8–31.3)	28.0 (24.4–32.1)	<0.001	25.9 (22.1–28.8)	31.8 (28.3–35.3)	<0.001
EAT volume indexed, mL/m^3	14.2 (11.8–19.9)	20.5 (18.3–23.8)	<0.001	18.7 (17.4–20.5)	23.9 (21.3–26.1)	<0.001

Continuous variables are expressed as the median with interquartile range for nonparametric variables. All the parameters of adipose tissue indexed to height^3. DMD, Duchenne muscular dystrophy; LGE, late gadolinium enhancement; PAAT, paracardial adipose tissue; EAT, epicardial adipose tissue; AVG, atrioventricular groove; IVG, interventricular groove; SAT, subcutaneous adipose tissue; PAT, pericardial adipose tissue.

Discussion

In this study, we demonstrated evidence that compared with healthy controls, patients with DMD had higher EAT deposition. The onset of LGE-based myocardial fibrosis was associated with EAT volume in patients with DMD. We then established a prediction model for the presence of myocardial fibrosis in patients with DMD using the nomogram, which included age, BFP, and EAT volume. The nomogram showed superior prediction performance with a high degree of calibration, discrimination, and clinical net benefit in the training and validation of DMD datasets. Therefore, the novel nomogram shows a potential for clinical use as a predictive marker of LGE-based myocardial fibrosis in DMD.

The increase of EAT may be related to many factors, such as fat replacement in the pathogenesis of DMD and fat redistribution caused by glucocorticoids. We further found that not only the EAT volume but also the EAT thickness and area in the local regions (such as the left AVG) in LGE-positive patients were higher than those in LGE-negative patients with DMD. Through paracrine signaling, EAT secretes a variety of inflammatory mediators, which may induce reactive fibrosis of the myocardial tissue (22,23). Therefore, we further hypothesized that EAT-related parameters might be useful for predicting LGE-based myocardial fibrosis in DMD. Consequently, we demonstrated that EAT volume was an independent risk factor for LGE positivity. In addition, previous studies

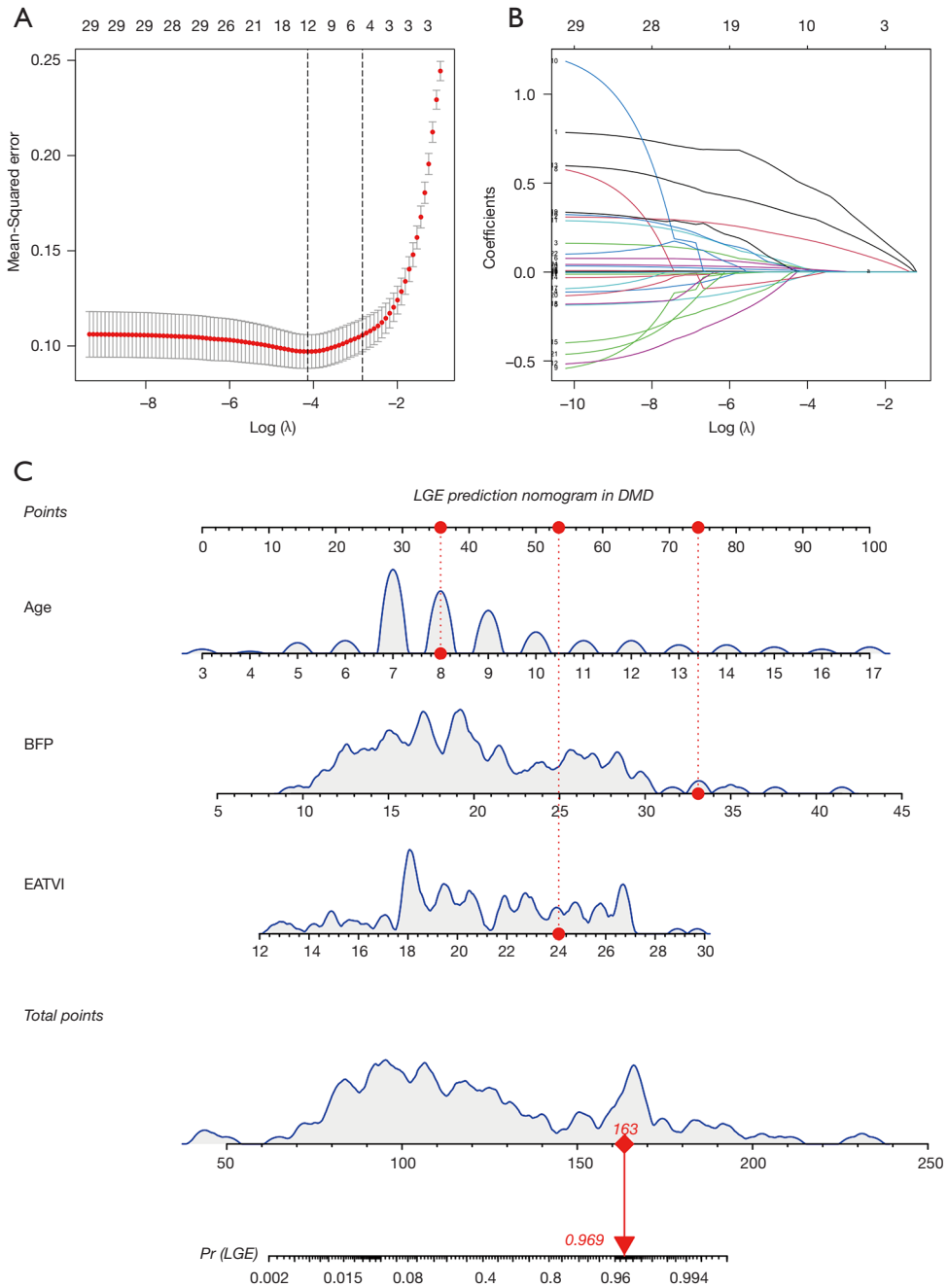

Figure 3 Nomogram to predict the occurrence of LGE-based myocardial fibrosis risk in DMD. (A) Tuning parameter lambda selection in the LASSO model used cross-validation for determining the minimal mean-squared error (the left dotted line) and the one standard error of the minimal mean-squared error (the right dotted line). (B) LASSO coefficient profiles of 29 variables were produced versus the log (lambda) sequence and 3 nonzero coefficient variables were selected. (C) Nomogram to predict myocardial fibrosis risk in DMD, with data taken from an 8-year-old child with DMD as an example. The steps for using the interactive dynamic nomogram are as follows: find the position of each risk factor on the corresponding axis (the higher blue wave crest indicates the more concentrated data distribution), draw a red dotted line to the points axis for the value of individual score, add the scores from the three risk factors, and finally draw a red solid line from the total point axis to determine the myocardial fibrosis probabilities of DMD. LGE, late gadolinium enhancement; DMD, Duchenne muscular dystrophy; BFP, body fat percentage; EATVI, epicardial adipose tissue volume indexed; LASSO, least absolute shrinkage and selection operator.

Table 3 Comparison of the predictors and LGE occurrence among all the sets

Parameter	DMD (n=283)			P value
	Training set (n=140)	Internal validation set (n=60)	External validation set (n=83)	
Age, years	8.8±2.8	8.7±2.6	8.9±2.9	0.982
BFP, %	19.1 (15.4–24.9)	19.6 (17.3–25.6)	17.9 (14.0–22.7)	0.101
EATVI, mL/m^3	20.5 (18.1–24.0)	21.0 (17.5–24.0)	20.5 (18.7–23.6)	0.953
LGE, n (%)	59 (42.1)	26 (43.3)	33 (39.8)	0.902

Continuous variables are expressed as the mean ± standard deviation for parametric variables or as the median with interquartile range for nonparametric variables. LGE, late gadolinium enhancement; DMD, Duchenne muscular dystrophy; BFP, body fat percentage; EATVI, epicardial adipose tissue volume indexed.

have found that left and right atrioventricular groove EAT thickness could contribute to diagnosis in patients with metabolic syndrome (21,24). In clinical practice, the local-region EAT thickness and area are easier to obtain than is the total volume of EAT. Therefore, we also analyzed the regional EAT thickness and area of patients with DMD. To avoid overfitting of the model, we used LASSO regression analysis to screen variables included in the prediction model to reduce the possible collinearity between parameters. However, due to the potentially high collinearity with EAT volume, the coefficients of local-region EAT thickness and area were compressed to zero in LASSO regression. Henson *et al.* found that BFP-based adiposity was independently associated with LGE-based myocardial fibrosis in DMD (5). Our study also found this association and confirmed these previous findings. Unexpectedly, both BFP and EAT volume, two parameters related to adipose tissue, were selected into the prediction model by the LASSO regression. In fact, EAT, which is composed of both brown and white adipocytes and maintains the potential for bidirectional transformation between brown and white adipose tissue (25,26), differs from subcutaneous adipose tissues and other visceral adipose tissues which are usually reflected by BFP (21,24). Therefore, we considered that there was no obvious collinearity between BFP and EAT volume in DMD. Interestingly, we observed that EAT volume showed a higher OR value than did BFP for predicting positive LGE in male children with DMD. This might be related to body fat reduction in some patients with DMD due to gastric dysfunction and malnutrition (27); furthermore, for patients with DMD and decreased cardiac function and water-sodium retention, the value of BFP measured by bioelectrical impedance analysis might be biased. Under the above specific conditions in patients with DMD, EAT volume may be more valuable in predicting the occurrence of myocardial fibrosis compared with BFP. Consistent with a previous study (5), age was also an independent risk factor for myocardial fibrosis in children with DMD in our study. For DMD patients, ages under 10 years old are defined as the preclinical stage, characterized by hypertrophy of myocardial cells, while ages over 10 years old are defined as the clinical stage, characterized by myocardial cell atrophy, apoptosis, and fibrosis (28). The previous study found that 52% of patients with DMD had LGE positivity on CMR, and the median age was 14.9 years (clinical stage) (5). Surprisingly, although the median age of the children with DMD was 8.0 years (preclinical stage) in our study, the incidence of LGE positivity on the first CMR was as high as 41.7%. In addition, we did not find any septal LGE positivity in isolation but in concurrence with other free wall segments of LGE positivity, which is consistent with previous studies (29). Myocardial fibrosis in children with DMD at the preclinical stage needs to be further investigated and the early use of CMR for evaluation. Notably, previous research has shown that cardiometabolic drugs, specifically sodium-glucose cotransporter-2 (SGLT2) inhibitors, have the potential to decrease EAT volume, resulting in improvements in inflammation and body weight (30). However, further research is necessary to determine whether the administration of relevant cardiometabolic medications in patients with DMD could effectively reduce EAT volume. This reduction in EAT volume might potentially contribute to the early prevention and intervention of myocardial fibrosis.

The three optimal predictors for LGE-based myocardial fibrosis in DMD were finally selected in the logistic regression equation. However, calculating the various probabilities using this mathematical formula was complicated and sometimes required computing equipment.

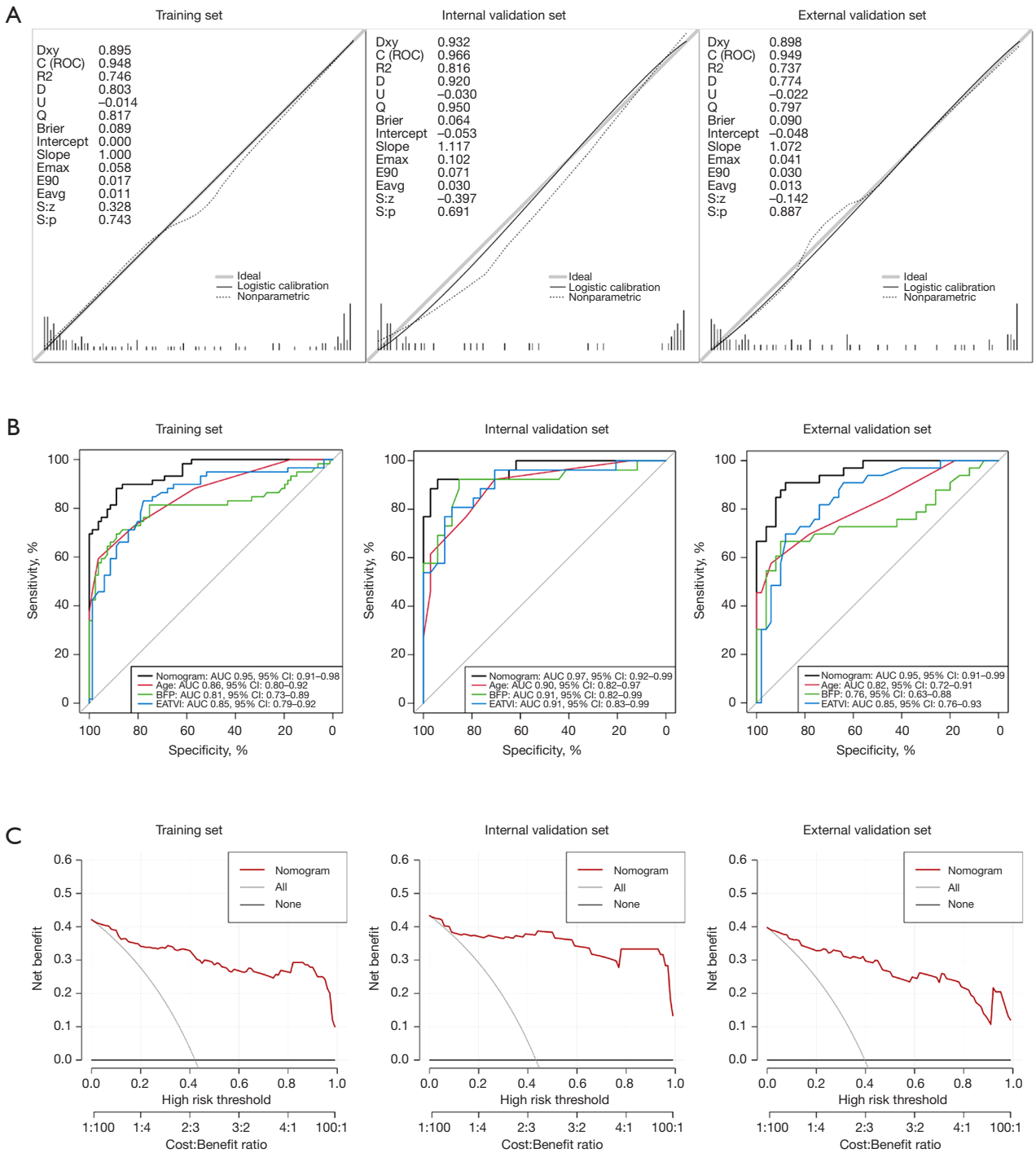

Figure 4 Development and validation of the nomogram. (A) Calibration plots evaluating the actual probability versus predicted probability of the nomogram in the training set, internal validation set, and external validation set. (B) The AUCs evaluating discrimination of the nomogram, age, BFP, and EAT volume in all sets. (C) Decision curve analysis reflecting the good clinical net benefit of the nomogram in all sets. DMD, Duchenne muscular dystrophy; BFP, body fat percentage; AUC, area under the curve; EATVI, epicardial adipose tissue volume indexed.

The interactive dynamic nomogram helped to simply visualize the prediction model and efficiently determine the myocardial fibrosis probability of each patient with DMD. The calibration plots showed the superior goodness of fit between the ideal lines and calibration lines, with fairly low Brier scores in this study. For the evaluation of discrimination in the nomogram, all the AUC values in the training and validation sets showed good performance and were higher than those of the single variable. Moreover, regardless of how the risk threshold probability changed, the net benefit maintained positive values in the decision curves, indicating good clinical applicability of the nomogram.

Our study has a few limitations that should be mentioned. First, we did not consider the cumulative dosing of glucocorticoids in our analysis; however, the duration of glucocorticoid administration was analyzed but not included in the prediction model in our study, which is in line with a previous study (5). Second, cardiac medications were not analyzed in our study. Third, EAT and BFP can be expected to increase together albeit not necessarily in a linear fashion, and the mechanisms of their interaction are difficult to elucidate at present. Fourth, we only assessed the positivity of LGE and did not evaluate the volume or mass of LGE. Fifth, this prediction model may be primarily applicable to patients with early-stage DMD, while it may not be suitable for those with late-stage DMD. Finally, our study did not account for differences in DMD genotypes.

Conclusions

Our study demonstrated a relationship between EAT deposition and myocardial fibrosis in patients with DMD. The occurrence of positive LGE was associated with an increased EAT volume. In addition, the nomogram with EAT volume showed superior performance in predicting the onset of LGE-based myocardial fibrosis in patients with DMD.

Acknowledgments

We thank Lu Zhang and Wei Bai (Department of Radiology, Key Laboratory of Obstetric and Gynecologic and Pediatric Diseases and Birth Defects of the Ministry of Education, West China Second University Hospital, Sichuan University, Chengdu, China) for their assistance with data collection.

Funding: This work was supported by the National Natural Science Foundation of China (No. 82271981), the Sichuan Science and Technology Program (Nos. 2021YFS0175 and 2023YFG0284), the Universal Application Project of Health Commission of Sichuan Province (No. 21PJ048), the Clinical Research Finding of Chinese Society of Cardiovascular Disease (CSC) of 2019 (No. HFCSC2019B01), and the Fundamental Research Funds for the Central Universities (No. SCU2020D4132).

Footnote

Reporting Checklist: The authors have completed the TRIPOD reporting checklist. Available at https://qims.amegroups.com/article/view/10.21037/qims-23-790/rc

Conflicts of Interest: All authors have completed the ICMJE uniform disclosure form (available at https://qims.amegroups.com/article/view/10.21037/qims-23-790/coif). X.Z. is an employee of Siemens Healthineers Digital Technology (Shanghai) Co., Ltd., Shanghai, China. X.B. is an employee of Siemens Medical Solutions USA, Inc., Los Angeles, CA, USA. The other authors have no conflicts of interest to declare.

Ethical Statement: The authors are accountable for all aspects of the work in ensuring that questions related to the accuracy or integrity of any part of the work are appropriately investigated and resolved. The study was conducted in accordance with the Declaration of Helsinki (as revised in 2013) and was approved by the China Ethics Committee of Registering Clinical Trials (ChiECRCT-20180107) and the Medical Ethics Committee of Sichuan University (No. K2019056). Informed consent was obtained from the patients' parents or their legal guardians.

References

1. Landfeldt E, Thompson R, Sejersen T, McMillan HJ,

Kirschner J, Lochmüller H. Life expectancy at birth in Duchenne muscular dystrophy: a systematic review and meta-analysis. Eur J Epidemiol 2020;35:643-53.
2. Mendell JR, Shilling C, Leslie ND, Flanigan KM, al-Dahhak R, Gastier-Foster J, Kneile K, Dunn DM, Duval B, Aoyagi A, Hamil C, Mahmoud M, Roush K, Bird L, Rankin C, Lilly H, Street N, Chandrasekar R, Weiss RB. Evidence-based path to newborn screening for Duchenne muscular dystrophy. Ann Neurol 2012;71:304-13.
3. Florian A, Ludwig A, Engelen M, Waltenberger J, Rösch S, Sechtem U, Yilmaz A. Left ventricular systolic function and the pattern of late-gadolinium-enhancement independently and additively predict adverse cardiac events in muscular dystrophy patients. J Cardiovasc Magn Reson 2014;16:81.
4. Schram G, Fournier A, Leduc H, Dahdah N, Therien J, Vanasse M, Khairy P. All-cause mortality and cardiovascular outcomes with prophylactic steroid therapy in Duchenne muscular dystrophy. J Am Coll Cardiol 2013;61:948-54.
5. Henson SE, Lang SM, Khoury PR, Tian C, Rutter MM, Urbina EM, Ryan TD, Taylor MD, Alsaied T. The Effect of Adiposity on Cardiovascular Function and Myocardial Fibrosis in Patients With Duchenne Muscular Dystrophy. J Am Heart Assoc 2021;10:e021037.
6. Packer M. Epicardial Adipose Tissue May Mediate Deleterious Effects of Obesity and Inflammation on the Myocardium. J Am Coll Cardiol 2018;71:2360-72.
7. Zeller J, Krüger C, Lamounier-Zepter V, Sag S, Strack C, Mohr M, Loew T, Schmitz G, Maier L, Fischer M, Baessler A. The adipo-fibrokine activin A is associated with metabolic abnormalities and left ventricular diastolic dysfunction in obese patients. ESC Heart Fail 2019;6:362-70.
8. Mahajan R, Kuklik P, Grover S, Brooks AG, Wong CX, Sanders P, Selvanayagam JB. Cardiovascular magnetic resonance of total and atrial pericardial adipose tissue: a validation study and development of a 3 dimensional pericardial adipose tissue model. J Cardiovasc Magn Reson 2013;15:73.
9. Nelson AJ, Worthley MI, Psaltis PJ, Carbone A, Dundon BK, Duncan RF, Piantadosi C, Lau DH, Sanders P, Wittert GA, Worthley SG. Validation of cardiovascular magnetic resonance assessment of pericardial adipose tissue volume. J Cardiovasc Magn Reson 2009;11:15.
10. Wong CX, Ganesan AN, Selvanayagam JB. Epicardial fat and atrial fibrillation: current evidence, potential mechanisms, clinical implications, and future directions. Eur Heart J 2017;38:1294-302.
11. Liu J, Li J, Pu H, He W, Zhou X, Tong N, Peng L. Cardiac remodeling and subclinical left ventricular dysfunction in adults with uncomplicated obesity: a cardiovascular magnetic resonance study. Quant Imaging Med Surg 2022;12:2035-50.
12. Silva MC, Meira ZM, Gurgel Giannetti J, da Silva MM, Campos AF, Barbosa Mde M, Starling Filho GM, Ferreira Rde A, Zatz M, Rochitte CE. Myocardial delayed enhancement by magnetic resonance imaging in patients with muscular dystrophy. J Am Coll Cardiol 2007;49:1874-9.
13. McDonald JS, McDonald RJ, Jentoft ME, Paolini MA, Murray DL, Kallmes DF, Eckel LJ. Intracranial Gadolinium Deposition Following Gadodiamide-Enhanced Magnetic Resonance Imaging in Pediatric Patients: A Case-Control Study. JAMA Pediatr 2017;171:705-7.
14. Mancio J, Pashakhanloo F, El-Rewaidy H, Jang J, Joshi G, Csecs I, Ngo L, Rowin E, Manning W, Maron M, Nezafat R. Machine learning phenotyping of scarred myocardium from cine in hypertrophic cardiomyopathy. Eur Heart J Cardiovasc Imaging 2022;23:532-42.
15. Puchalski MD, Williams RV, Askovich B, Sower CT, Hor KH, Su JT, Pack N, Dibella E, Gottliebson WM. Late gadolinium enhancement: precursor to cardiomyopathy in Duchenne muscular dystrophy? Int J Cardiovasc Imaging 2009;25:57-63.
16. Bushby K, Finkel R, Birnkrant DJ, Case LE, Clemens PR, Cripe L, Kaul A, Kinnett K, McDonald C, Pandya S, Poysky J, Shapiro F, Tomezsko J, Constantin C; . Diagnosis and management of Duchenne muscular dystrophy, part 1: diagnosis, and pharmacological and psychosocial management. Lancet Neurol 2010;9:77-93.
17. Ledesma-Carbayo MJ, Kellman P, Hsu LY, Arai AE, McVeigh ER. Motion corrected free-breathing delayed-enhancement imaging of myocardial infarction using nonrigid registration. J Magn Reson Imaging 2007;26:184-90.
18. Gaborit B, Jacquier A, Kober F, Abdesselam I, Cuisset T, Boullu-Ciocca S, Emungania O, Alessi MC, Clément K, Bernard M, Dutour A. Effects of bariatric surgery on cardiac ectopic fat: lesser decrease in epicardial fat compared to visceral fat loss and no change in myocardial triglyceride content. J Am Coll Cardiol 2012;60:1381-9.
19. Gaborit B, Kober F, Jacquier A, Moro PJ, Cuisset T, Boullu S, Dadoun F, Alessi MC, Morange P, Clément K, Bernard M, Dutour A. Assessment of epicardial fat volume

and myocardial triglyceride content in severely obese subjects: relationship to metabolic profile, cardiac function and visceral fat. Int J Obes (Lond) 2012;36:422-30.
20. Flüchter S, Haghi D, Dinter D, Heberlein W, Kühl HP, Neff W, Sueselbeck T, Borggrefe M, Papavassiliu T. Volumetric assessment of epicardial adipose tissue with cardiovascular magnetic resonance imaging. Obesity (Silver Spring) 2007;15:870-8.
21. Liang KW, Tsai IC, Lee WJ, Lee IT, Lee WL, Lin SY, Wan CJ, Fu CP, Ting CT, Sheu WH. MRI measured epicardial adipose tissue thickness at the right AV groove differentiates inflammatory status in obese men with metabolic syndrome. Obesity (Silver Spring) 2012;20:525-32.
22. Anthony SR, Guarnieri AR, Gozdiff A, Helsley RN, Phillip Owens A, Tranter M. Mechanisms linking adipose tissue inflammation to cardiac hypertrophy and fibrosis. Clin Sci (Lond) 2019;133:2329-44.
23. Cherian S, Lopaschuk GD, Carvalho E. Cellular cross-talk between epicardial adipose tissue and myocardium in relation to the pathogenesis of cardiovascular disease. Am J Physiol Endocrinol Metab 2012;303:E937-49.
24. Wang TD, Lee WJ, Shih FY, Huang CH, Chang YC, Chen WJ, Lee YT, Chen MF. Relations of epicardial adipose tissue measured by multidetector computed tomography to components of the metabolic syndrome are region-specific and independent of anthropometric indexes and intraabdominal visceral fat. J Clin Endocrinol Metab 2009;94:662-9.
25. Sacks HS, Fain JN, Bahouth SW, Ojha S, Frontini A, Budge H, Cinti S, Symonds ME. Adult epicardial fat exhibits beige features. J Clin Endocrinol Metab 2013;98:E1448-55.
26. Dozio E, Vianello E, Briganti S, Fink B, Malavazos AE, Scognamiglio ET, Dogliotti G, Sigrüener A, Schmitz G, Corsi Romanelli MM. Increased reactive oxygen species production in epicardial adipose tissues from coronary artery disease patients is associated with brown-to-white adipocyte trans-differentiation. Int J Cardiol 2014;174:413-4.
27. Zou X, Ouyang H, Pang D, Han R, Tang X. Pathological alterations in the gastrointestinal tract of a porcine model of DMD. Cell Biosci 2021;11:131.
28. D'Amario D, Amodeo A, Adorisio R, Tiziano FD, Leone AM, Perri G, Bruno P, Massetti M, Ferlini A, Pane M, Niccoli G, Porto I, D'Angelo GA, Borovac JA, Mercuri E, Crea F. A current approach to heart failure in Duchenne muscular dystrophy. Heart 2017;103:1770-9.
29. Hor KN, Taylor MD, Al-Khalidi HR, Cripe LH, Raman SV, Jefferies JL, O'Donnell R, Benson DW, Mazur W. Prevalence and distribution of late gadolinium enhancement in a large population of patients with Duchenne muscular dystrophy: effect of age and left ventricular systolic function. J Cardiovasc Magn Reson 2013;15:107.
30. Myasoedova VA, Parisi V, Moschetta D, Valerio V, Conte M, Massaiu I, Bozzi M, Celeste F, Leosco D, Iaccarino G, Genovese S, Poggio P. Efficacy of cardiometabolic drugs in reduction of epicardial adipose tissue: a systematic review and meta-analysis. Cardiovasc Diabetol 2023;22:23.

Cite this article as: Yuan W, Xu H, Yu L, Wen L, Xu K, Xie L, Xu R, Fu H, Liu B, Xu T, Zhou X, Bi X, Cai X, Guo Y. Association of increased epicardial adipose tissue derived from cardiac magnetic resonance imaging with myocardial fibrosis in Duchenne muscular dystrophy: a clinical prediction model development and validation study in 283 participants. Quant Imaging Med Surg 2024;14(1):736-748. doi: 10.21037/qims-23-790

Supplementary

Appendix 1 Two-sample *t*-test power analysis

Numeric results for the two-sample t test

Null hypothesis: mean1 = mean2. Alternative hypothesis: mean 1 < mean 2
The standard deviations were assumed to be unknown and unequal.

Power	N1	N2	Ratio	Alpha	Beta	Mean 1	Mean 2	S1	S2
0.90352	57	285	5	0.05	0.09648	14.3	15.8	3.1	5.0

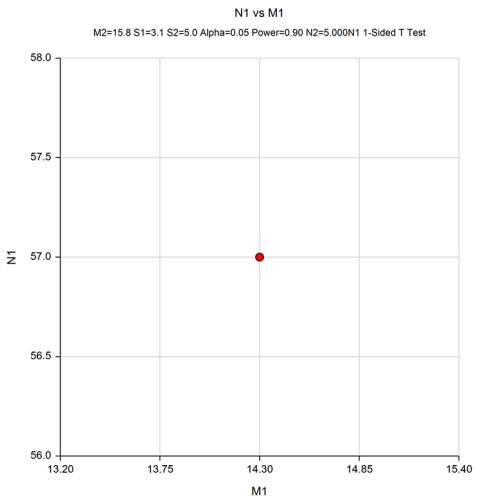

Report definitions

Power is the probability of rejecting a false null hypothesis. Power should be close to one.
N1 and N2 are the number of items sampled from each population. To conserve resources, they should be small.
Alpha is the probability of rejecting a true null hypothesis. It should be small.
Beta is the probability of accepting a false null hypothesis. It should be small.
Mean 1 is the mean of populations 1 and 2 under the null hypothesis of equality.
Mean 2 is the mean of population 2 under the alternative hypothesis. The mean of population 1 is unchanged.
S1 and S2 are the population standard deviations. They represent the variability in the populations.

Summary statements

Group sample sizes of 57 and 285 achieve 90% power to detect a difference of –1.5 between the null hypothesis that both group means are 14.3 and the alternative hypothesis that the mean of group 2 is 15.8 with estimated group standard deviations of 3.1 and 5.0 and with a significance level (alpha) of 0.05000 according to a one-sided two-sample t test.

References

1. Machin D, Campbell MJ, Fayers PM, Pinol APY. Sample Size Tables for Clinical Studies, 2nd Edition. Blackwell Science. Malden, MA, 1997.
2. Zar JH. Biostatistical Analysis (Second Edition). Prentice-Hall. Englewood Cliffs, New Jersey, 1984.

https://dx.doi.org/10.21037/qims-23-790

Table S1 Intraclass correlation coefficients for quantitative parameters of different adipose tissues

Parameter	Intraobserver		Interobserver	
	ICC	(95% CI)	ICC	(95% CI)
PAAT thickness indexed, mm/m^3	0.88	(0.81, 0.93)	0.83	(0.73, 0.90)
EAT thickness indexed, mm/m^3				
Left AVG	0.94	(0.90, 0.96)	0.89	(0.82, 0.94)
Right AVG	0.83	(0.72, 0.89)	0.89	(0.82, 0.93)
Anterior IVG	0.87	(0.80, 0.92)	0.84	(0.75, 0.90)
Superior IVG	0.86	(0.78, 0.92)	0.79	(0.67, 0.87)
Inferior IVG	0.82	(0.71, 0.89)	0.84	(0.75, 0.90)
Right ventricular free wall	0.76	(0.63, 0.85)	0.78	(0.66, 0.87)
SAT thickness indexed, mm/m^3	0.91	(0.85, 0.94)	0.92	(0.86, 0.95)
PAAT area indexed, mm^2/m^3	0.90	(0.84, 0.94)	0.89	(0.82, 0.93)
EAT area indexed, mm^2/m^3				
Left AVG	0.91	(0.86, 0.95)	0.93	(0.89, 0.96)
Right AVG	0.88	(0.81, 0.93)	0.87	(0.79, 0.92)
Anterior IVG	0.92	(0.87, 0.95)	0.92	(0.87, 0.95)
Superior IVG	0.87	(0.79, 0.92)	0.91	(0.85, 0.94)
Inferior IVG	0.93	(0.89, 0.96)	0.92	(0.88, 0.95)
Right ventricular free wall	0.89	(0.82, 0.93)	0.88	(0.81, 0.93)
PAT volume indexed, ml/m^3	0.88	(0.81, 0.93)	0.85	(0.76, 0.91)
EAT volume indexed, ml/m^3	0.92	(0.87, 0.95)	0.90	(0.83, 0.94)

All the parameters of adipose tissue indexed to height^3. ICC, intraclass correlation coefficient; CI, confidence interval; PAAT, paracardial adipose tissue; EAT, epicardial adipose tissue; AVG, atrioventricular groove; IVG, interventricular groove; SAT, subcutaneous adipose tissue; PAT, pericardial adipose tissue.

https://dx.doi.org/10.21037/qims-23-790